CATTLE PRACTICE ISSN 0969-1251
2025 33(4)

DOI Link: https://doi.org/10.59671/J6232
Vol.33, Issue.4, Part.1, April 2025, PP.2-21

Green synthesis, characterization, antibacterial and antioxidant activity of Ag/ZnO Nanoparticles

Fawzeeh N. Alharbi [1], Fatima A.S. Al-Yusufy [1], Zulfa M. Abaker [1,] *, Suzan Zein Alabdeen Makawi [1], Hamdoon A. Mohammed[2], Tasneem I. Hussein [1] and Ebtesam Hassan Lutf Alhamzi[3]

[1] Department of Chemistry, College of Science, Qassim University, Saudi Arabia.
[2] Department of Medicinal Chemistry and Pharmacognosy, College of Pharmacy, Qassim University, Saudi Arabia.
[3] Department of Biology, Faculty of Science, Sana'a University, Yemen.

*Corresponding Author:
Zu.Ahmed@qu.edu.sa

Received Feb 2025 Accepted March 2025 Published April 2025

Abstract: Using *Artemisia absinthium* leaf extract, an eco-friendly approach was employed to synthesize silver-doped zinc oxide nanoparticles (Ag/ZnO NPs). The synthesized (NPs) were characterized using Fourier transform infrared (FTIR) spectroscopy, X-ray diffraction (XRD), and surface area (BET). The FTIR showed the absorption peak of the (Zn-O) bond between 400 and 450 cm^{-1}. The XRD revealed a decrease in particle size from 18.77 to 16.07 nm and an increase in the BET from 6.032 to 12.151 m^2/g for the green and Ag/ZnO NPs, respectively. The antibacterial activity was tested against three types of bacteria strains, *Staphylococcus aureus* ATCC 6538, *Bacillus subtilis* ATCC 6633, and *Pseudomonas aeruginosa* ATCC 9027, at different volumes (5, 10, 20, and 30 µL). The Ag/ZnO NPs showed more enhanced antibacterial activity than the green ZnO NPs and higher than the gentamycin antibiotic. The antioxidant activity of the NPs was assessed using three different assays. Doping ZnO NPs with Ag increased their reducing power in both ferric reducing antioxidant power (FRAP) and total antioxidant activity (TAA) assays; however, green ZnO NPs scavenged free radicals (DPPH) more effectively than Ag/ZnO NPs. Finally, this study highlights the successful green synthesis of Ag/ZnO NPs, revealing that the NPs' smaller particle sizes and larger surface area significantly enhanced their antibacterial activity.

Keywords: Green synthesis; *A. absinthium*; Ag/ZnO NPs; antioxidant; antibacterial activity; gentamycin.

1. Introduction

In recent years, the study of NPs has emerged as one of the significant basic fields in the biomedical sciences[1]. Among several routes of NP synthesis, the green synthesis method has been reported as an environmentally friendly approach[2]. Researchers concentrate on the environmentally friendly synthesis of NPs from various plant components, including leaves, fruits, seeds, roots, stems, and microorganisms, including bacteria, algae, fungi, and yeast, for multiple uses. Green NPs made from plants are more stable and possess a wider range of sizes and shapes than other organisms. By limiting the exposure and use of costly and harmful chemicals, the green synthesis strategy increases catalytic activity and controlled particle form and size, which are essential factors in a variety of biomedical applications and also protect the environment from dangerous chemicals[3].

The majority of plants are naturally capable of reducing and capping a variety of metal and metal oxide NPs, yet some are more capable than others because they contain unique phytochemical components that are crucial to the bio-reduction process and the subsequent creation of NPs[3,4]. *A. absinthium* plant extract was employed as a reducing and stabilizing agent as a straightforward, economical method as well as a substitute for conventional preparation techniques for the production of different types of NPs. *A. absinthium*, also known as wormwood, is a significant perennial shrubby medicinal plant that is indigenous to Asia, the Middle East, Europe, and North Africa and widely found in the United States and Canada, with about 500 – 800 species categorized as annual, perennial, and biennial natural plants or tiny shrubs,While few Artemisia species are toxic and allergic weeds, many are economically and pharmacologically significant since they are used as antioxidant and anticancer, antimicrobial, and medicinal products, as well as aesthetics, feedstuffs, fodder, and soil binder[5].

Due to two significant limitations, ZnO is generally regarded as a non-viable material for practical applications. The first limiting factor is ZnO's larger bandgap (3.37 eV), which limits its response to UV light only. The second is photoexcited charge carrier fast recombination. These limitations have been partially overcome by mixing these oxides with noble metals to extend the plasmonic effect's absorption into the visible spectrum, enhancing their performance. These minerals have been doped with ZnO to produce low bandgap materials, such as Cu, Ti, Ru, Bi and Ag[6–10]. The doping process involves introducing a specific ion not present in the original material into a crystal lattice. Ag is the ideal noble metal for doping ZnO NPs, and it enhances its characteristics, such as surface area, band gap reduction, and morphological modification, resulting in increased antibacterial activity[10].

According to recent publications, ZnO NPs have shown biological uses in medication administration, gene transfer, and bio imprinting. They also possess antibacterial, antifungal, antidiabetic, and anticorrosive properties[11,12]. The Ag/ZnO and green

ZnO NPs are better than conventional antibiotics because they affect bacteria directly through various mechanisms, including bacterial cell membrane penetration, bacterial cell disruption, and inhibiting transcription, translation, and replication. Furthermore, some NPs, such as Ag, have a greater affinity for phosphorus and sulfur, which causes them to bond specifically with macromolecules containing phosphorus, such as DNA and RNA, and membrane proteins containing sulfur. Sulfur breaks down nucleic acids and prevents protein synthesis, which disrupts the regular operation of the bacterial cell and leads to its death[13,14].

The Ag/ZnO and green ZnO NPs are also used as antioxidants. The antioxidants enable the body to combat free radicals. Free radicals are a typical byproduct of cellular metabolism, and they are produced alongside reactive oxygen species (ROS) regularly in our cells. Disruption of the equilibrium between endogenous defence mechanisms and ROS, or free radicals, is known as oxidative stress. The formation of ROS can increase when in a diseased state [15,16]. The two primary categories of antioxidant activity measurement techniques are colourimetric and non-colourimetric. The most widely used and straightforward colourimetric techniques are (DPPH), (TAA) and (FRAP) assays, whereas the hydroxyl radical scavenging assay (HRSA) is a non-colourimetric technique. The time-effectiveness, affordability, and simplicity of the DPPH assay make it a popular choice. The reaction mechanism in the DPPH assay is based on electron transfer. However, this is based on scavenging organic radicals (DPPH radicals)[17].

The novelty of this work is synthesizing Ag/ZnO NPs using the *A. absinthium* plant extract. The *A. absinthium* plant extract was selected based on the number of bioactive chemicals essential for stabilizing and reducing Ag onto the ZnO lattice, forming Ag/ZnO NPs with improved biological uses in addition to non-toxic, environmentally safe, inexpensive, and easy to use. Ag ion was chosen to dope with the ZnO lattice because it is highly poisonous to bacteria; it also exhibits antibacterial abilities by binding to the bacterial cell membrane and disrupting cellular respiration. This study's primary purpose is to produce green Ag/ZnO NPs using *A. absinthium* plant extract and to evaluate their antibacterial efficiency against the Gram-positive ATCC 6538 and ATCC 6633 and Gram-negative ATCC 9027 bacteria and to assess their antioxidant activities using three different assays; DPPH, TAA and FRAP. High-quality Ag/ZnO NPs with efficient structural and morphological features have been manufactured to meet this need. The NPs were verified using FTIR, XRD, BET and DLS analysis.

2. Materials and Methods

Chemical and reagents

The plant materials as aerial parts were collected in February 2021 from private gardens in Al-Rass City, Qassim, Saudi Arabia. Zinc nitrate hexahydrate ($Zn(NO_3)_2 \cdot 6H_2O$) was purchased from LOBA Chemie, potassium hydroxide (KOH) from Techno Pharmchem, Bahadurgarh, India, and silver nitrate ($AgNO_3$) from Alfa Aesar company, Ward Hill, Massachusetts, United States. The Artemisia absinthum leaf extract and all the solutions were prepared using deionized water. DPPH radical, FRAP and TAA (Tokyo Chemical Industry Co., Ltd. (TCI), Tokyo, Japan) were sourced from Egypt. Dimethyl sulfoxide (DMSO 99%) was purchased from Sigma-Aldrich, Milwaukee, United States. Mueller–Hinton Agar was purchased from Hi-media, Mumbai, India. The tested bacteria strains, ATCC 6538, ATCC 6633, and ATCC 9027, were obtained from Yemen Standardization, Metrology and Quality Control Organization, Sana'a, Yemen.

Preparation of *A. absinthium* extract/synthesis of green ZnO NPs.

Our previously published paper mentioned the preparation of *A. absinthium* extract and green ZnO NP [18].

Synthesis of Ag/ZnO NPs

An ultrasound sonicator was used to synthesize Ag/ZnO NPs by reducing Ag^+ ions to Ag^0 on the surface of ZnO using *A. absinthium* extract as the reducing agent. A volume of 90 mL of (0.34 M) aqueous solution of $Zn(NO_3)_2 \cdot 6H_2O$ and an amount of KOH (0.5M) were added to adjust pH to 12. While sonicating at 500 Hz, 90 mL of (0.06 M) of $AgNO_3$ solution was added for doping, and 10 mL of *A. absinthium* extract as a reducing agent was added. The reaction took 30 min to complete, and finally, a light grey residue (Ag/ZnO) was obtained, centrifuged, and rinsed several times with deionized water, then dried in a hot air oven at 90 °C. The powder was calcined at 500 °C in a muffle furnace for 2 h under atmospheric conditions (figure 1). This method was adapted from Aliannezhadi et al. with a few modifications[19].

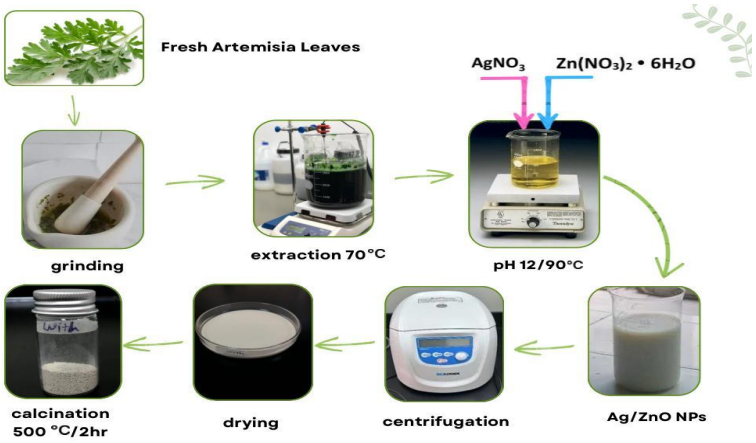

Figure 1: A schematic representation of green synthesis of the Ag/ZnO NPs using *A. absinthium* extract.

Characterization of Ag/ZnO NPs

The KBr technique was employed to determine the functional groups using the Shimadzu Fourier transform infrared spectrophotometer (FTIR, 4000–400 $cm^{-1)}$, fixed path length, Kyoto, Japan). An X-ray diffractometer (XRD, Rigaku, Tokyo-Japan, with K beta filter, time duration 10.000°/min, scanning range 10.0–90.0°, and operated at 40 kV, 40 mA) was used to verify the crystal size examination. The widely recognized Scherrer formula was used to calculate the average crystal size, *D*[20]:

$$D = \frac{K\lambda}{\beta \,.\cos\theta} \qquad (1)$$

K is a constant equal to 0.90; λ is the wavelength (0.154 nm); β is the full width at half maximum (FWHM) in radians; and ϑ is the diffraction angle. Surface properties and pore size were determined by nitrogen desorption measured at 77 °C using a NOVA 2200e surface area analyzer (Anton Paar Quanta Tec Inc., Boynton Beach, FL, USA) Dynamic light scattering (DLS) was used to determine PSD, (PDI), and ZP of the prepared Ag/ZnO and green ZnO NPs using Malvern Zetasizer (version 5.10), United Kingdom.

Surface area (BET) determination

The surface characteristics and pore size distribution of the Ag/ZnO NP were determined through nitrogen physisorption. A surface area analyzer determined nitrogen adsorption and desorption isotherms at 77 °K. About 0.3g of the Ag/ZnO NP powder was placed in the tube and was allowed to be degassed in a vacuum for at

least three hrs. at 160 °C before the measurement was made. Using the adsorption data at P/Po 0.05-0.25, the specific surface area (SBET) was computed using the Brunauer-Emmett-Teller (BET) method, and the pore size distribution and pore volume were obtained from the adsorption branch using the Barrett-Joyner-Halenda (BJH) model. At a relative pressure P/Po of 0.992, the total pore volume (V_{total}) was calculated from the amount of adsorbed material[21].

Antibacterial Activity

The antibacterial activity assays of the Ag/ZnO and green ZnO NPs were carried out using the hole plate diffusion method[22]. Three Petri dishes were pre-inoculated with the appropriate bacteria in the following manner:
A volume of 100 µL of the bacterial suspension was spread over plates containing Mueller–Hinton agar using a sterile cotton swab. Three wide holes (with diameters of 5 mm) were then made in the agar using a cork borer. The synthesized NPs solutions of the concentration (0.1 µg/µl) in DMSO were prepared. Different volumes of the prepared solutions (5 µL, 10 µL, 20 µL, and 30 µL) were then introduced into each of the holes in appropriately labelled Petri dishes using a sterile micropipette. Gentamycin (10 µg/mg) was used as a positive control. The dishes were then incubated at 37 °C for 24 h, after which the zones of inhibition (ZOIs) were measured and recorded. The ZOI was taken to be the diameter of the zone, visibly showing the absence of growth, including the 5 mm well. If there was no inhibition, a value of 0 mm was assigned to the test sample. The experiments were carried out in triplicates, and the mean and standard deviation were calculated.

Antioxidant Activity

The antioxidant activity of the prepared nanoparticles was measured using three different in vitro assays, including the radical scavenging effect (DPPH), reduction of the molybdenum (VI) ions (TAA), and the reduction of ferric ions (FRAP). All these assays were conducted in triplicate, and the results were expressed as the means of all measurements with their standard deviations.

DPPH assay

The preparation of the DPPH stock and working solutions was conducted according to the literature [23]. 1 mL of the DPPH solution (6 mg in 50 mL of methanol) was mixed with 1 mL of the samples' solution in DMSO containing 0.2 mg of the samples. After 30 min of the dark incubation, the absorbances were taken at 517 nm. The DPPH scavenging effect of the samples was calculated as mg equivalent to standard Trolox.

TAA assay

The TAA was measured as reported by Abdellatif et al. [24]. In this essay, 2 mL of the fresh molybdenum (VI) reagent was added to the sample solution (2 mL containing 0.2 mg of the samples). The absorbances of the mixtures were recorded after 45 min

of the water bath heating at 90 °C. The TAA of the samples was measured as mg-trolox equivalent.

FRAP assay

The method was proceeded according to Aroua et al. [25]. 0.2 mg of the samples in 0.1 mL of the solvent were added to 2 mL of the freshly prepared FRAP reagent, which was prepared as described in the literature [26]. The absorbances were recorded at 593 nm after 30 min of the dark incubation, and the results were expressed as a mg Trolox equivalent.

3. Results and Discussion

FTIR Analysis

Figure 2 depicts the infrared spectra of the *A. absinthium* extract and Ag/ZnO NPs. The IR spectra of the *A. absinthium* show absorption peaks at 3410, 2937, 1705, 1610, and 1063 $cm^{-1,}$ which correspond to the stretching modes of O–H, C–H sp^3, C=O, C=C, and C–O groups, respectively, suggesting the presence of alcohol, phenolic and flavonoid constituents found in the *A. absinthium* leaf extract. When comparing the Ag/ZnO NPs spectra to the plant spectrum, there was a noticeable drop in the peak's intensity at about 3400 cm^{-1}. The polyphenol-rich biomolecules that possess OH functional groups are essential in reducing the NPs. The new broad absorption band in the 400 – 450 cm^{-1} range attributed to the Zn-O bond for the Ag/ZnO NPs, which confirmed their formation. These results are in line with those of previous studies[27].

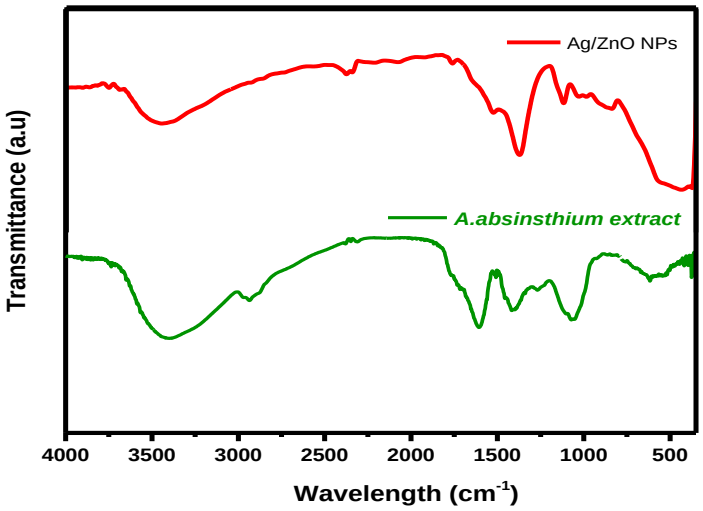

Figure 2: FTIR spectra of Ag/ZnO NPs in comparison to *A. absinthium* extract

XRD Analysis

Figure 3 displays the diffractograms of the Ag/ZnO NPs. The nanoparticles showed a hexagonal wurtzite phase, with no evidence of peak impurity or a secondary phase compared to the JCPDS Card No. 01-072-5089 data. Sharp and narrow diffraction peaks, in particular, (100), (002), and (101), exhibit excellent crystal structure and peak intensities. Sharp extreme peaks for the Ag/ZnO NP appear at 2θ values of 31.84°, 34.49°, 36.33°, 47.62°, 56.69°, 62.95°, 66.51°, 68.03°, and 69.17°, corresponding to the planes of the following orientations: (100), (002), (101), (102), (110), (103), (200), (112), and (201), respectively.

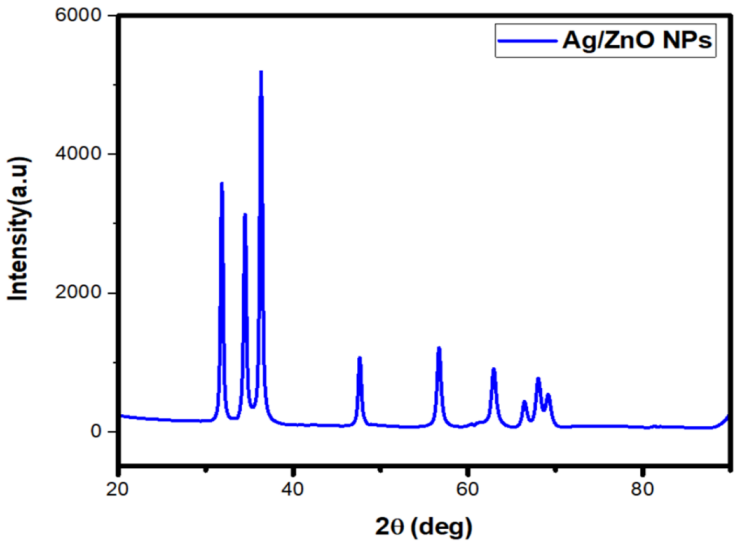

Figure 3: XRD diffractograms of Ag/ZnO NPs

The Ag/ZnO NPs' crystallite size was calculated from the XRD data using the Scherrer formula, represented by Equation (1) and presented in Table 1. The value for the Ag/ZnO NPs is 16.07 nm, whereas for green, NPs was 18.77nm. (Determined in the previously published paper[18]). A subsequent crystallite size decrease was observed when the ZnO NPs were doped with Ag ions. The fixation of Ag ions on the surface of the ZnO NPs may be responsible for reducing the particle size, which in turn slows down the ZnO crystal structure's subsequent growth[28,29].

Table 1: Crystallite size of Ag/ZnO NPs

No. of Peaks	indices	2θ	FWHM	Size(nm)
1	100	31.8465	0.3903	21.18
2	002	34.4985	0.4061	20.49
3	101	36.3335	0.4076	20.52
4	102	47.6265	0.4739	18.33
5	110	56.6942	0.5888	15.34
6	103	62.9586	0.6868	13.57
7	200	66.5170	0.8695	10.93
8	112	68.0396	0.7386	12.98
9	201	69.1743	0.8489	11.37
			Average size	**16.07**

BET Determination

The precise surface area of the Ag/ZnO NPs was determined using BET. Table 2 and Figure 4 display the BET, pore volume, and average pore diameter. The isotherm confirmed the typical Type IV behaviour of ZnO NPs, which is represented by a deceleration loop in the low-pressure region (P/P0 < 0.8), typical of mesoporous NPs. The calculated BET was 12.151 (m^2/g), where the pore volume was 0.046 (cm^3/g). The addition of silver caused an increase in the BET values of the ZnO NPs. Since the Ag/ZnO NPs showed a large surface area, the material's behaviour began to be dominated by its surface qualities[30]. The common Barrett-Joyner- Halenda (BJH) pore size distribution curves show that most mesoporous particles have a size of less than 40 nm.

Table 2: BET, pore volume, and pore distribution of Ag/ZnO and green ZnO NPs.

Samples	BET (m^2/g)	Pore Volume (cm^3/g)	Average Pore Diameter (nm)	Ref.
Green ZnO NPs	6.032	0.017	15.876	[18]
Ag/ZnO NPs	12.151	0.046	15.882	This work

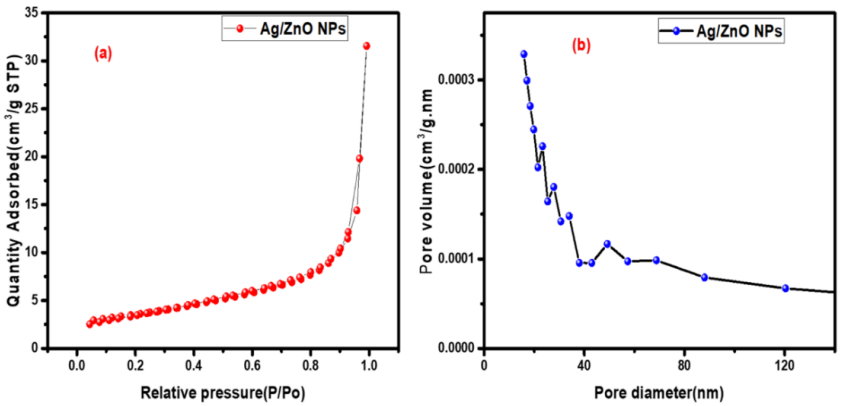

Figure 4: a) N_2 adsorption-desorption isotherms and b) pore size distribution of Ag/ZnO NPs

Particle size distribution (PSD) and zeta potential (ZP) evaluation

The hydrodynamic particle size distribution and zeta potential analysis of the Ag/ZnO and green ZnO NPs were measured by DLS. The higher the ZP, the more stable the particles are and the less likely they are to form agglomerates because of the repulsion of the counter ions of the particle surfaces. The Z-average particle size and the ZP surface charge are illustrated in Figures 5 and 6. The Ag/ZnO NPs results revealed three notable peaks indicating polydisperse particles with a Z-average size of 772.7 nm, a ZP of 8.83 mV, and a PDI of 0.381. In contrast, the green ZnO NPs displayed a nearly monodisperse particle nature with a hydrodynamic size of 674 nm, ZP of -8.89 mV, and PDI of 0.400. The ZP values of the Ag/ ZnO and green ZnO NPs suggest moderate repulsive forces, increasing the likelihood of the NPs' aggregation[31]. According to the previous study[32], the positively charged NPs showed the highest bactericidal activity, whereas the negatively charged NPs had the least antibacterial activity. The antibacterial efficacy of NPs depends on the electrostatic interaction between their positively charged particles and negatively charged bacterial cells. From the obtained results, Ag/ZnO NPs had higher antibacterial activity.

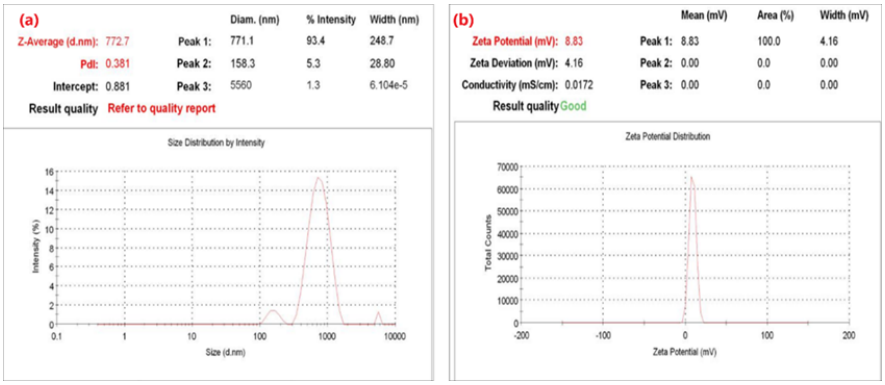

Figure 5: DLS analysis (a) PSD by intensity (b) Zeta Potential of Ag/ZnO NPs.

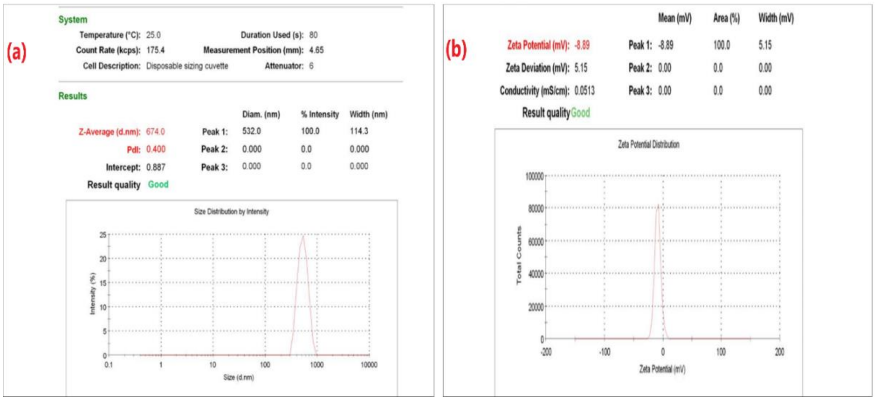

Figure 6: DLS analysis (a) PSD by intensity (b) Zeta Potential of green ZnO NPs.

Antibacterial Activities

The antibacterial activity of Ag/ZnO and green ZnO NPs against both Gram-positive (*Staphylococcus aureus* ATCC 6538 and *Bacillus subtilis* ATCC 6633) and Gram-negative (*Pseudomonas aeruginosa* ATCC 9027) bacteria was investigated using zone inhibition methods[22]. The antibacterial activity of Ag/ZnO and green ZnO NPs against the bacteria mentioned above is presented in Figure 7. The ZOI around the sample-impregnated disk increased with an increasing sample solution level, indicating the bactericidal potential of the test compounds. The ZOI values of Ag/ZnO

and green ZnO NPs NPs against *S. aureus, B. subtilis, and P. aeruginosa* are tabulated in Table 3. Based on the obtained results, Ag/ZnO and green ZnO NPs showed enhanced antibacterial activity. The Ag/ZnO NPs showed a dramatic increase (about 2-fold) in their antibacterial activity compared to the green ZnO NPs against all the tested bacteria. The antibacterial activities of the Ag/ZnO NPs were even higher than those of gentamycin (as a standard tablet). The enhanced antibacterial activity was explicitly due to Ag ions anchored to the ZnO nanostructure[32].

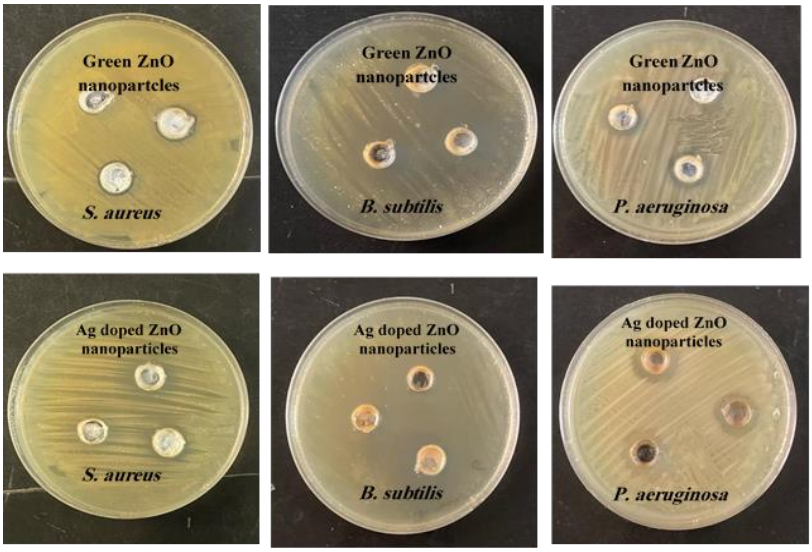

Figure 7: Antibacterial activities of Ag/ZnO and green ZnO NPs synthesized using *A. absinthium* extract.

Table 3: Antibacterial activities of the synthesized Ag/ZnO and green ZnO NPs against *Staphylococcus aureus* ATCC 6538, *Bacillus subtilis* ATCC 6633, and *Pseudomonas aeruginosa* ATCC 9027 bacteria at different solution levels, with gentamycin antibiotic as a control.

No.	Sample	(µL)	Bacteria Strain		
			S. aureus	*B. subtilis*	*P. aeruginosa*
			ZOI (mm)		
1	Ag/ZnO NPs	10	1.33 ± 0.58	10.0 ± 1.00	2.67 ± 0.58
		20	2.00 ± 0.00	11.67 ± 0.58	4.33 ± 0.58
		30	3.33 ± 0.58	14.33 ± 0.58	6.0 ± 1.00
2	Green ZnO NPs	10	0	4.67 ± 0.58	0
		20	1.33 ± 0.58	7.33± 0.58	1.0 ± 0.00
		30	1.67 ± 0.58	8.0 ± 1.00	2.33 ± 0.58
3	DMSO[a]	10	0	0	0
4	Gentamycin[b] (µg/mg)	-	2.33 ± 0.58	10.33 ± 0.58	0

[a] negative control; [b] positive control. The data presented as mean ± SD of three independent experiments performed in triplicates.

Findings from previous studies[33,34] have suggested a correlation exists between the antibacterial activity and physicochemical characteristics (such as particle size, morphology, and surface defects) of ZnO NPs. Studies have indicated that particle size is essential for improving antibacterial effect. The smaller the particle size, the better the antibacterial activity. The diameter of the peptidoglycan layer in both Gram-positive and negative bacteria cell walls is on the nanometer scale. The smaller the particle size, the more easily it can interact with the cell wall and cause damage[35]. When comparing the particle size and surface defects of the ZnO NPs, the Ag/ZnO NPs showed the smallest particle size with the largest surface and surface defects due to the interstitial incorporation of the Ag ions into the ZnO nanostructure. Hence, the enhanced antibacterial activity of the Ag/ZnO NPs is supported.

Ag/ZnO and green ZnO NPs are more effective against bacteria due to their capacity to bind and enter bacterial cells. The investigation of the antibacterial properties of ZnO NPs and the precise mechanism of their toxicity remains inadequately comprehended and is a topic of debate. Additional elaboration is necessary to address various inquiries about the range of antibacterial efficacy. Multiple modes of action, including the effects on the bacterial cell wall and membrane, contribute to the antibacterial activities of ZnO NPs against *S. aureus, B. subtilis*, and *P. aeruginosa*[14]. These effects can be explained by various mechanisms, such as oxidative stress caused by the production of reactive oxygen species(ROS), damage to the integrity of

cell membranes of bacteria, and the release of Zn^{2+} and Ag^{+} ions that disrupt crucial cellular function, which finally leads to the cell death. Generally, Ag/ZnO and green ZnO NPs can produce Zn^{2+} and Ag^{+} ions that penetrate bacterial cells and interfere with essential metabolic processes such as enzyme activity and DNA replication, leading to differences in antibacterial effectiveness against various bacterial strains[35]. A possible antibacterial mechanism for Ag/ZnO and green ZnO NPs is shown in Figure 8.

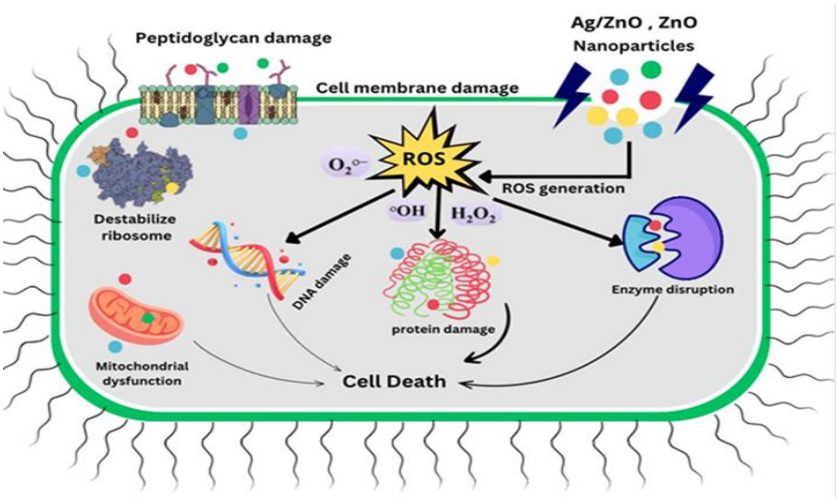

Figure 8: A schematic representation of the antibacterial mechanism of Ag/ZnO and green ZnO NPs

Antioxidant Activity

The antioxidant activity of a possible antibacterial mechanism for Ag/ZnO and green ZnO NPs was determined using three common in vitro assays. The NPs were tested for their ability to scavenge free radicals, such as DPPH, and reduce transition metals, such as molybdenum (VI) to molybdenum (V) and Fe^{3+} to Fe^{2+}. The role of free radical scavengers in human health and food safety is well established[15]. Also, reducing the amount of transition metals reduces oxidative stress because metal ions contribute to ROS production via the Fenton and Haber-Weiss reactions[36]. The antioxidant activity of the Ag/ZnO and green ZnO NPs is presented in Table 4. and expressed as the mean results of three measurements with the standard deviations. The results express the antioxidant activity of all samples; however, variations between them in

different methods might be reflected in their activities against free radicals and in reducing the transition metals. The DPPH test showed that the green ZnO NPs had a higher free radical scavenging effect (6.54 ± 0.07 mg Trolox equivalent) than the Ag/ZnO NPs (5.60 ± 0.02 mg Trolox equivalent). These results indicated that the green synthesis of ZnO NPs enhanced the free radical scavenging of the compound; however, Ag/ZnO NPs reduced its activity (Table 4).

On the other hand, green ZnO NPs were the lowest metal-reducing active samples compared to Ag/ZnO NPs. In addition, the Ag/ZnO NP was enhancing the reducing power. The lower radical scavenging effect of Ag/ZnO NPs compared to green ZnO NPs could be attributed to the concentration of Ag/ZnO NPs, which have been shown to have lower activity at higher concentrations than at lower concentrations. In that context, Robkhob et al. reported that 2% of Ag/ZnO NPs had a higher free radical scavenging effect than 4% [37]. However, Ag/ZnO NPs have enhanced the reducing power of the green ZnO NPs, but the results are inconsistent with the literature.

Table 4: Antioxidant activity of Ag/ZnO and green ZnO NPs

Samples	(DPPH) *	(TAA)*	(FRAP)*
Ag/ZnO NPs	5.60 ± 0.02	6.44 ± 0.14	6.42 ± 0.07
Green ZnO NPs	6.54 ± 0.07	5.66 ± 0.08	5.92 ± 0.05

*The measurements were conducted in triplicate and calculated as mg Trolox equivalent.

4. Conclusions

Ag/ZnO NPs were successfully synthesized through an eco-friendly route using the bioactive *A. absinthium* leaf extract as a reducing and stabilizing agent. The prepared Ag/ZnO NPs were characterized using XRD, FTIR, BET and DLS. The particle size of Ag/ZnO was 16.07 nm, smaller than that of green ZnO NPs, which was found to be 18.77 nm. The FTIR results showed a drop in the peak's intensity at about 3400 cm^{-1}, possessing OH functional groups for polyphenol and the new broad absorption bands noticed for Ag/ZnO NPs around the 400–450 cm^{-1} range characteristic of Zn-O bond. The addition of silver caused an increase in the BET value compared to the calculated BET value of green ZnO NPs. The surface area was 12.151, 6.032 (m^2/g), the pore volume was 0.046 (cm^3/g), and 0.017 for Ag/ZnO and green ZnO NPs, respectively. DLS measured the PSD, ZP and PDI; the values were 772.7 and 674nm, 8.83 and -8.89,

0.381and 0.400 for Ag/ZnO and green ZnO NPs, respectively. Ag/ZnO NPs showed higher antibacterial activity due to electrostatic interaction between positively and negatively charged bactericidal cells.
Antibacterial activity of synthesized Ag/ZnO NPs against the three bacterial strains, *Staphylococcus aureus* ATCC 6538, *Bacillus subtilis* ATCC 6633, and *Pseudomonas aeruginosa* ATCC 9027showed an enhanced antibacterial efficacy compared to the green ZnO NPs, precisely due to the silver ions anchored to the ZnO NPs disrupting cellular respiration, leading to the death of the bacteria.
Regarding antioxidant activity, the results revealed that while green ZnO NPs were more effective at scavenging free radicals, Ag/ZnO NPs improved their reducing power, highlighting the complex interplay between the NP's composition and their antioxidant activity.
Based on the results, we can conclude that A. absinthium leaf extract offers a potential source of bioactive compounds for eco-friendly synthesis of the NPs, replacing chemical methods[5]. The synthesized Ag/ZnO and green ZnO NPs using *A. absinthium* leaf extract in their low concentrations (0.1 μg/μl) were active against the growth of the test bacteria strains. Therefore. In addition, the Ag/ZnO NPs showed antibacterial activity even higher than the gentamycin antibiotic [10], which may serve as potential antibacterial agents for future use.

Acknowledgements: The authors are grateful for the technical support of the Chemistry Department at the College of Science, Qassim University.

Conflicts of Interest: The authors declare no conflicts of interest.

References

1. kazemi S, Hosseingholian A, Gohari SD, Feirahi F, Moammeri F, Mesbahian G, et al. Recent advances in green synthesized nanoparticles: from production to application. Mater Today Sustain. 2023;24:100500.

2. Ying S, Guan Z, Ofoegbu PC, Clubb P, Rico C, He F, et al. Green synthesis of nanoparticles: Current developments and limitations. Environ Technol Innov. 2022;26:1–20.

3. Bawazeer S. Green synthesis of silver nanoparticles from Euphorbia milii plant extract for enhanced antibacterial and enzyme inhibition effects. Int J Health Sci (Qassim). 2024;18:25–32.

4. Osman AI, Zhang Y, Farghali M, Rashwan AK, Eltaweil AS, Abd El-Monaem EM, et al. Synthesis of green nanoparticles for energy, biomedical, environmental, agricultural,

and food applications: A review. Environ. Chem. Lett. 2024.

5. Aida MS, Alonizan N, Zarrad B, Hjiri M. Influence of plant extract on the homogeneous and heterogeneous green chemistry synthesis of nanostructured ZnO. J Taibah Univ Sci [Internet]. 2023;17. Available from: https://doi.org/10.1080/16583655.2023.2179819

6. Sowjanya B, King P, Vangalapati M, Myneni VR. Copper-Doped Zinc Oxide Nanoparticles : Synthesis , Characterization , and Application for Adsorptive Removal of Toxic Azo Dye. Int J Chem Eng. 2023;2023.

7. Pinzari F. Synthesis, Photocatalytic and Bio Activity of ZnO-TiO2 Nanocomposites: A Review Study. Reactions. 2024;5:680–739.

8. Micaela RP, Belén S, Ana U, Paloma F. Ruthenium-doped ZnO nanostructures: Growth, characterization, and applications in waveguides and light-emitting devices. Ceram Int. 2024;50:43788–99.

9. Sermsrithong C, Jaidaew P, Promjantuk C, Buabthong P. Structural and Optical Properties of Bismuth-doped ZnO Nanoparticles Synthesized by Co-precipitation. Int J Eng Trans C Asp. 2022;35:2344–9.

10. Gonfa MH, Birhanu AL. Green Chemistry Letters and Reviews Green synthesis , characterization and antibacterial evaluation of ZnO and Ag-doped ZnO nanoparticles using Ruta chalepensis leaf extract. Green Chem Lett Rev [Internet]. 2024;17:1–14. Available from: https://doi.org/10.1080/17518253.2024.2412613

11. Mendes CR, Dilarri G, Forsan CF, Moraes V De, Sapata R, Renato P, et al. Antibacterial action and target mechanisms of zinc oxide nanoparticles against bacterial pathogens. Sci Rep. 2022;12:1–10.

12. Rahimi G, Mohammad KS, Zarei M, Shokoohi M, Oskoueian E, Poorbagher MR, et al. Zinc oxide nanoparticles synthesized using Hyssopus Officinalis L . Extract Induced oxidative stress and changes the expression of key genes involved in inflammatory and antioxidant Systems. Biol Res. 2022;55:1–10.

13. More PR, Pandit S, Filippis A De, Franci G, Mijakovic I, Galdiero M. Silver Nanoparticles : Bactericidal and Mechanistic Approach against Drug-Resistant Pathogens. Microorganisms. 2023;11.

14. Hamdy E, Al-askar AA, El-gendi H, Khamis WM, Behiry SI, Valentini F, et al. Zinc Oxide Nanoparticles Biosynthesized by Eriobotrya japonica Leaf Extract :

Characterization, Insecticidal and Antibacterial Properties. Plants. 2023;12:1–15.

15. Chandimali N, Bak SG, Park EH, Lim H, Won Y, Kim E. Free radicals and their impact on health and antioxidant defences : a review. Cell Death Discov [Internet]. 2025;11:2025. Available from: http://dx.doi.org/10.1038/s41420-024-02278-8

16. Jomova K, Raptova R, Alomar SY, Alwasel SH, Nepovimova E, Kuca K, et al. Reactive oxygen species, toxicity, oxidative stress, and antioxidants : chronic diseases and ageing. Arch Toxicology. 2023;97:2499–574.

17. Christodoulou MC, Palacios JCO, Hesami G, Jafarzadeh S, Lorenzo JM, Moreno A, et al. Spectrophotometric Methods for Measurement of Antioxidant Activity in Food and Pharmaceuticals. Antibiotics. 2022;11.

18. Alharbi FN, Abaker ZM, Makawi SZA. Phytochemical Substances — Mediated Synthesis of Zinc Oxide. Inorganics. 2023;11:1–14.

19. Aliannezhadi M, Mohamadi FD, Jamali M. Ultrasound-assisted green synthesized ZnO nanoparticles with different solution pH for water treatment. Sci Rep. 2025;15:1–17.

20. Fatimah S, Ragadhita R, Fitria D, Husaeni A, Bayu A, Nandiyanto D. How to Calculate Crystallite Size from X-ray diffraction (XRD) using Scherrer Method. ASEAN J Sci Eng [Internet]. 2022;2:65–76. Available from: http://ejournal.upi.edu/index.php/AJSE/

21. Jowkar Z, Moaddeli A, Hamidi SA. Synthesis and characterization of mesoporous zinc oxide nanoparticles and evaluation of their biocompatibility in L929 fibroblasts. Clin Exp Dent Res. 2024;10:1–11.

22. El-Fallal AA, Elfayoumy RA, El-Zahed MM. Antibacterial activity of biosynthesized zinc oxide nanoparticles using Kombucha extract. SN Appl Sci. 2023;5:332.

23. Mohammed HA. Phytochemical Analysis, Antioxidant Potential, and Cytotoxicity Evaluation of Traditionally Used Artemisia absinthium L.(Wormwood) Growing in the Central Region of Saudi Arabia. Plants. 2022;11:1028.

24. Abdellatif AAH, Mohammed HA, Abdulla MH, AL-SUBAIYEL AM, Mahmood A, Samman WA, et al. Green synthesized silver nanoparticles using the plant-based reducing agent Matricaria chamomilla induce cell death in colorectal cancer cells. Eur Rev Med Pharmacol Sci. 2023;27:10112–25.

25. Aroua LM, Almuhaylan HR, Alminderej FM, Messaoudi S, Chigurupati S, Al-Mahmoud S, et al. A facile approach synthesis of benzoylaryl benzimidazole as potential α-amylase and α-glucosidase inhibitor with antioxidant activity. Bioorg Chem. 2021;114:105073.

26. Mohammed HA, Ali HM, Qureshi KA, Alsharidah M, Kandil YI, Said R, et al. Comparative Phytochemical Profile and Biological Activity of Four Major Medicinal Halophytes from Qassim Flora. Plants. 2021;10:2208.

27. Pasieczna-patkowska S, Cichy M. Application of Fourier Transform Infrared (FTIR) Spectroscopy in Characterization of Green Synthesized Nanoparticles. Molecules. 2025;30:1–36.

28. Makauki E, Mtavangu SG, Basu OD, Rwiza M, Machunda R. Facile biosynthesis of Ag–ZnO nanocomposites using Launaea cornuta leaf extract and their antimicrobial activity. Discov Nano [Internet]. 2023;18. Available from: https://doi.org/10.1186/s11671-023-03925-2

29. Iqbal Y, Raouf Malik A, Iqbal T, Hammad Aziz M, Ahmed F, Abolaban FA, et al. Green synthesis of ZnO and Ag-doped ZnO nanoparticles using Azadirachta indica leaves: Characterization and their potential antibacterial, antidiabetic, and wound-healing activities. Mater Lett. 2021;305.

30. Babayevska N, Przysiecka Ł, Iatsunskyi I, Nowaczyk G, Jarek M, Janiszewska E, et al. ZnO size and shape effect on antibacterial activity and cytotoxicity profile. Sci Rep [Internet]. 2022;12:1–13. Available from: https://doi.org/10.1038/s41598-022-12134-3

31. Singh P, Mijakovic I. Strong Antimicrobial Activity of Silver Nanoparticles Obtained by the Green Synthesis in Viridibacillus sp . Extracts. Front Microbiol. 2022;13:1–13.

32. Johnson D, Reeks JM, Caron A, Tzoka I, Ali I, McGillivray SM, et al. Influence of Surface Properties and Microbial Growth Media on Antibacterial Action of ZnO. Coatings. 2022;12.

33. Okeke IS, Agwu KK, Ubachukwu AA, Ezema FI. Influence of transition metal doping on physiochemical and antibacterial properties of ZnO[sbnd]Nanoparticles: A review. Appl Surf Sci Adv. 2022;8.

34. Babayevska N, Przysiecka Ł, Iatsunskyi I, Nowaczyk G, Jarek M, Janiszewska E, et al. ZnO size and shape effect on antibacterial activity and cytotoxicity profile. Sci Rep. 2022;12:8148.

35. Sampath S, Bhushan M, Saxena V, Pandey LM. Green synthesis of Ag doped ZnO nanoparticles : study of their structural , optical , thermal and antibacterial properties. Mater Technol [Internet]. 2022;37:2785–94. Available from: https://doi.org/10.1080/10667857.2022.2075307

36. Aroua LM, Alosaimi AH, Alminderej FM, Messaoudi S, Mohammed HA, Almahmoud SA, et al. Synthesis , Molecular Docking , and Bioactivity Study of Novel Hybrid Benzimidazole Urea Derivatives : A Promising α -Amylase and α -Glucosidase Inhibitor Candidate with Antioxidant Activity. Pharmaceutics. 2023;15.

37. Robkhob P, Ghosh S, Bellare J, Jamdade D, Tang I-M, Thongmee S. Effect of silver doping on antidiabetic and antioxidant potential of ZnO nanorods. J Trace Elem Med Biol. 2020;58:126448.